A block-movement-based analysis for cohesive powders in a rotating drum experiment

T. Kronlachner [a,b], S. Pirker [b], T. Lichtenegger [b,*]

[a] K1-MET Metallurgical Competence Center, Stahlstraße 14, 4020 Linz, Austria
[b] Department of Particulate Flow Modelling, Johannes Kepler University, Altenberger Str. 69, 4040 Linz, Austria

ARTICLE INFO

ABSTRACT

The precise characterization of the flow behavior of cohesive powders can be challenging. With the block-movement-based analysis, we introduce a more immediate characterization technique that even works for highly cohesive powders. Based on the strongly discontinuous dynamics in rotating drums dominated by the formation of large blocks and their subsequent breakage in abrupt avalanche events, it describes the flow behavior with geometrical properties of the falling down structures like block height or speed. Its advantages are the higher information content and the short observation time to get stable results. These properties make it a promising candidate for calibrating parameters for computer simulations. In addition, its high sensitivity allows to detect even small changes in the flow behavior. We demonstrate the method with three metal powders and identify the differences in their flowability. Furthermore, we investigate the influence of preconditioning at different humidity to underline the sensitivity of our approach.

© 2022 The Author(s). Published by Elsevier B.V. This is an open access article under the CC BY license (http://creativecommons.org/licenses/by/4.0/).

1. Introduction

Characterization of granular materials based on small samples is essential for understanding and/or predicting the qualitative bulk behavior and consequently for handling and processing of the substance. It also allows to identify external influence factors (e.g. humidity) and quantify their impact. Furthermore, detailed computer simulations rely on high-fidelity material parameters to be extracted from characterization procedures.

For powders, small grain sizes cause the cohesive attraction forces to dominate the dissipative interaction between the individual particles. This allows them to form stable blocks which behave almost like rigid bodies, which makes the measurement of the bulk flow characteristics more challenging. To determine such properties, several standard test procedures are established [1], but for highly cohesive powders, these experiments do not give enough information to adequately characterize the flow behavior, or they simply do not work at all. Due to the increasing interest in a deeper understanding of these materials, also pushed by the growing importance of additive manufacturing, a lot of research on the characterization of cohesive powders in various consolidation states has been conducted in the last few years [2–5]. The region for medium

to high consolidation is covered well with direct shear testing equipment. The most prominent are the Jenike shear cell [6], the Ring-Shear Tester [7], and the direct shear device for the FT4 powder rheometer [8]. The FT4 powder rheometer also provides a test for the low consolidation stress region, where it uses propeller blades to measure the energy needed for motion. In-house tests showed that especially with highly cohesive powders, this method exhibited strong fluctuations, which made it difficult for us to determine material properties with high fidelity.

Instead, we chose to use a rotating-drum setup which is useful both for cohesionless [9,10] and for cohesive [4,11] granular systems. Notably, these tests are not limited to a single run like the heap experiments. Rather, the granular flow can be investigated continuously. The behavior of the material depends heavily on the rotational speed. In the regime with continuous motion of the granular material, the angle that establishes at the interface between material and air is comparable to the angle of repose from the heap experiments. Therefore, it is often called dynamic angle of repose [2,11–14]. Besides this angle, there are additional ways of characterizing the behavior of powder in a rotating drum. Lumay et al. [2] used an evaluation method based on the interface between material and air. In addition to the angle, they also retained the deviation around the mean interface, because cohesive powders show a less continuous flow behavior but are rather dominated by avalanches (which either shear slide, wall slide, or slump [14]) with sizes comparable to the interface deviation. In the case of extremely cohesive powders, the bed rotates initially with the drum until it has reached a

* Corresponding author.
E-mail addresses: tobias.kronlachner_1@jku.at (T. Kronlachner), stefan.pirker@jku.at (S. Pirker), thomas.lichtenegger@jku.at (T. Lichtenegger).

Nomenclature

Latin of symbols

D	Diameter
L	Length

List of abbreviations

AM	Additive Manufacturing
DEM	Discrete Element Method
PIV	Particle Image Velocimetry
RH	Relative Humidity

critical angle which can be close to an overhang. Then, an avalanche breaks away from the dense powder bed in the form of a rigid-looking block.

This peculiarity has become the topic of several investigations ranging from questions regarding how to best detect such avalanches to their interpretation in terms of material properties. Image-based methods like particle tracking velocimetry (PTV) can be used to compute the velocity field in the cross-section and hence to identify avalanches [9,15]. Alternatively, Davis et al. [16] employed a load cell to determine the change of the center of gravity for sensing motion, and they showed that avalanches could be recognized with this technique. While Pleass et al. [17] studied the avalanche angle as an indication for flow properties, Trpělková et al. [18] focused on the involved energies. They introduced the avalanche break energy, i.e. the potential energy gained before an avalanche occurs in comparison to the starting state, as an additional parameter to the common avalanche energy that describes the potential energy released through the avalanche. These works point out very clearly that the avalanche behavior provides key information for characterizing cohesive materials.

Given the intricate behavior of this type of target system, we can identify some properties of high interest for a material characterization procedure to be used for subsequent calibration simulations: (i) The method should provide as much information about the powder behavior as possible because one cannot expect that fitting of a single DEM parameter will capture the complex dynamics. Instead, several parameters need to be optimized simultaneously necessitating large amounts of data. (ii) It should be easily reproducible by numerical simulations to facilitate optimization. (iii) Furthermore, the faster the characterization can give stable and reliable results, the less time a corresponding simulation has to run within an optimization loop to find the best fitting contact parameters.

With these requirements in mind, we have another look at the characterization methods for cohesive powders in a low-stress consolidation state. The interface evaluation method provides only two values (the mean interface angle and the deviation around the mean interface) to capture the flow behavior at one specific rotation speed, where the latter can be seen as a measure for the cohesiveness of the particles. The measurement of avalanche energies reveals information about the strength of cohesive forces, too, but suffers from a low information rate. Each avalanche only provides one energy value, which necessitates a large number of them to get reliable statistics. Additionally, in order to precisely analyze the energy values, the rotation rate has to be quite low. Taken together, these two factors imply long observation periods both in the experiment and, more importantly, in corresponding calibration simulations. To gain more information, different rotation speeds may be used. However, measurement times would rise drastically and a larger number of simulation runs would have to be carried out for the various angular frequencies.

To overcome the difficulties described above, in particular the need for long time series, and to capture as much of the flow properties as possible, we propose a more immediate way to describe the behavior of cohesive materials. An avalanche in a rotating drum basically occurs when the shear in a plane exceeds what the material can withstand. This depends on the height of the material over the shear plane and its angle, which constitute two important characterization parameters that we monitor continuously in our drum. For this analysis, the velocity in the cross-section is extracted via image processing to precisely identify and measure all events. We primarily focus on the geometric properties of the down-falling blocks. This provides us with information about the complex flow behavior caused by strong cohesive forces. Because the block-movement-based method does not only get one-shot information per avalanche but instead investigates the avalanche behavior during the whole process starting from the breakaway down to the point of falling apart, a lot fewer avalanches have to be recorded.

Our paper is organized as follows: In Section 2, we describe the methodology, starting with the block evaluation method in Sec. 2.1 followed by the interface evaluation method in Sec. 2.2. In Section 3, the experimental setup is described. The characterization of two different cohesive metal powders with very small grain sizes is reported in Sec. 4, where we present results for fixed and varying rotational speed. We demonstrate the capabilities of the method in indicating changes in the powder flowability by using preconditioned material. Furthermore, we show that it works for the simpler case of mildly cohesive materials as well by using a third powder exhibiting weaker cohesive forces. Finally, we compare the results of our approach with the interface analysis method along the lines of Lumay et al. [2]. We conclude our manuscript with a thorough discussion and an outlook on the next steps in our research agenda in Sec. 5.

2. Explanation of methods

In the following, we introduce our novel analysis method based on automatically identified blocks and their properties. In a second subsection, we describe an approach that makes use of the interface between powder and air and especially its behavior. This is comparable to the technique of Lumay et al. [2] for the rotating drum.

2.1. Block-like movement evaluation method

We developed an evaluation method for rotating drum experiments that targets the block-like movement of cohesive powders. It focuses on the characterization of the blocks that break away from the rigid-like moving powder bed. Therefore, the velocity field of the powder relative to the drum is analyzed for moving structures, which is done by digital image analysis. Since the drum can only be examined at the cover, we have to assume that the material behavior does not change too much along the axis.

The method can be decomposed into four steps: velocity field estimation in the cross-section, detection of blocks, characterization of the blocks, and evaluation of the distribution of these values. Fig. 1 visualizes the process starting from two frames to the block detection and evaluation. In the following, these steps are described in more detail.
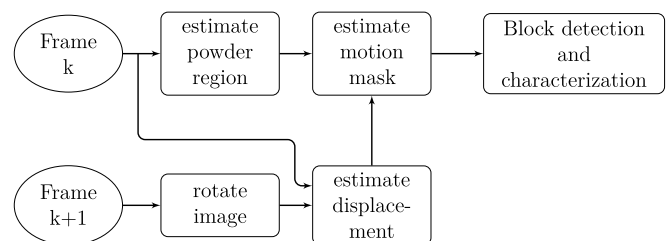

Fig. 1. Flowchart of the block evaluation method. It shows how two consecutive frames (k and k + 1) are prepared for the block detection and characterization.

2.1.1. Velocity field estimation in the cross-section of the drum

The velocity field can be approximated by calculating the displacement between two consecutive frames and dividing it by the time between the two frames. For the estimation of the displacement, the images need to be prepared. First, the video clip of an experimental run is split into individual frames and the drum is detected in the first frame of the video with the help of the Hough transformation [19]. The frames are cropped such that the drum is image filling, resulting in images where the center of the drum and the image match. After the image preprocessing, the velocity in the cross-section at the front surface is estimated with the help of a neural network from image pairs. The second image of each pair is corrected for the known rotation of the drum via the rotation matrix

$$M = \begin{pmatrix} \cos(\omega\Delta t) & -\sin(\omega\Delta t) \\ \sin(\omega\Delta t) & \cos(\omega\Delta t) \end{pmatrix} \qquad (1)$$

with the angular velocity of the drum ω and the time between frames Δt. M is applied on the second frame of each pair to get the rotated image img_{rot} with the affine transformation

$$img_{rot}(x,y) = img(M_{11}x + M_{12}y, M_{21}x + M_{22}y) \qquad (2)$$

which uses linear interpolation in the source image (img). Consequently, only motion relative to the drum is registered by the subsequent velocity estimation.

The neural network 'ScopeFlow' (https://github.com/avirambh/ScopeFlow) from Bar-Haim et al. [20] is employed with a pre-trained checkpoint in inference mode. The architecture of this network is based on the PWC-Net [21] and the iterative refinement (IRR) processing introduced by Hur & Roth [22]. The PWC architecture uses two consecutive frames, from which feature maps at different levels are created by convolutional filters. A warping process of the second image's features is used to account for large motion at each level using the upsampled flow from the coarser level. Subsequently, a correlation operation is applied, and the flow is estimated at each level by a CNN decoder. With the IRR adoption, only one shared decoder for all pyramid levels is used. The estimation of the optical flow is given by the post-processed output of the decoder at the finest level.

Neural-network-based optical flow estimation turned out to be necessary because conventional methods like particle image velocimetry (PIV) [23] or the Lucas–Kanade approach for dense optical flow estimation [19] could not provide data of sufficient quality.

2.1.2. Detection of powder moving as block

Blocks are detected based on the estimated displacements to the next frame as well as the visual image of the experiment. First, the visual image is used to identify which areas of the drum are covered with powder. This can be done by a simple threshold on the visual image because the bright LED backlight separates the powder well from the background, as shown in Fig. 2. After the creation of the so-called powder
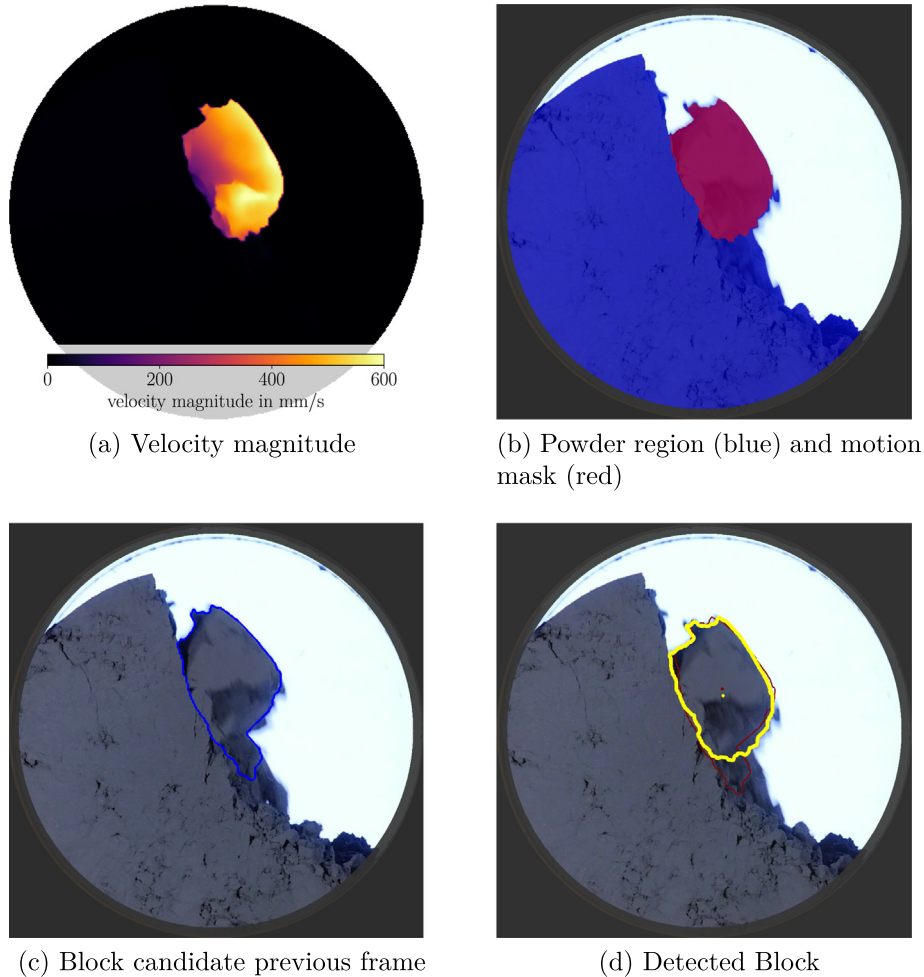

(a) Velocity magnitude

(b) Powder region (blue) and motion mask (red)

(c) Block candidate previous frame

(d) Detected Block

Fig. 2. Illustration of the block detection algorithm. The estimated velocity magnitude relative to the drum (a) and the visual image are used to identify the powder and motion regions (b). The former is obtained by thresholding the visual image, and the latter is given by the velocity field above a certain threshold. A block is detected by using a block candidate from a previous frame (c), which is transformed and compared (red in (b)) to the current frame (d) and used to identify the block (yellow).

region, the velocity field, displayed in Fig. 2a, is masked with this domain to guarantee that the velocity is zero in regions where no powder is situated. This velocity field is then masked with a minimum velocity threshold $v_{min}=40$ mm s^{-1} to create the so-called motion mask which is highlighted in Fig. 2b. The velocity threshold is limited from below by the precision of the setup and the quality of the velocity estimation. The chosen threshold is a trade-off between the margin to the lower limit and the risk of missing slow blocks. The motion mask can consist of multiple regions, e.g. one block moving down the powder bed and the other breaking away at the top.

For the detection of blocks, we segment the motion mask into connected areas called contours which are monitored over time. A contour is detected as block when it can be found in at least two consecutive frame pairs and meets the following detection criteria. First, an affine transformation with the restriction of having no scaling and no shear is fit to the displacement data of a contour in the first frame pair. The contour recognized in the first frame pair (see Fig. 2c) is then transformed correspondingly and compared to the contour in the second frame pair according, position, area, and shape (see Fig. 2d). For each occurrence of a block, its area, mean velocity, direction, height, and width are registered. These measurements are described in more detail in the following section. An example of a block detected in this way can be seen in Fig. 2d.

2.1.3. Characteristic values for a detected block

In order to implement the previously mentioned idea with the height above the shear layer, two length measurements are used to get a representative value for the block size. The block width is defined in direction of and the height perpendicular to the mean velocity. To reduce the influence of peaks which would significantly affect the overall size measurement, we define these lengths such that 98% of the corresponding area lie inside of them. For the block speed, the mean of the velocity field over the block contour is calculated. More specifically, the block speed is defined as the magnitude of the mean velocity and the direction of the block is defined as the angle of the mean velocity

vector. According to Wojtkowski et al. [14], blocks can occur in two different ways, shear sliding and slumping. To distinguish between these behaviors, the rotation of the velocity field is calculated and averaged over the block contour. In the first case, there is nearly no rotation of the block due to sliding, compared to the second case where the block starts rotating when it breaks away from the powder bed. To further characterize the stability of the rigid-like moving powder bed, the top edge of each block is registered. Sketches of the measured values are provided in Table 1, an example of block height and direction measurement is shown in Fig. 3.

2.1.4. Distributions of the measured block values

For the final evaluation of the described parameters, distribution functions are calculated. Additionally, the values are weighted with the detected block area so that the histogram represents the distribution with regard to the amount of powder in motion. For the measurements reported in this study, we used histograms with fixed bin count and range collected in Table 1.
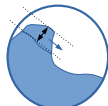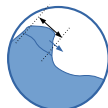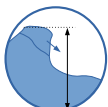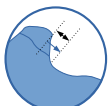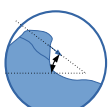
2.1.5. Visual filling ratio

To quantify the filling of the drum, the visual filling degree is introduced as an additional measure. It describes how much of the cross-section is occupied by powder. The area of the powder region described in the previous section is divided by the area of the full circle resulting in a value from 0 to 1. The filling degree is also measured over time and evaluated with a histogram like the block-based parameters. Under the assumption that the surface is relatively flat along the direction of the rotational axis, it can be used to evaluate the bulk density of the powder during the rotation of the drum.

2.2. Interface evaluation method

The interface evaluation method is based on the interface between the powder and the air extracted from the visual images. These interfaces are analyzed with regard to the mean angle and the deviation

Table 1
Ranges for histogram evaluation.

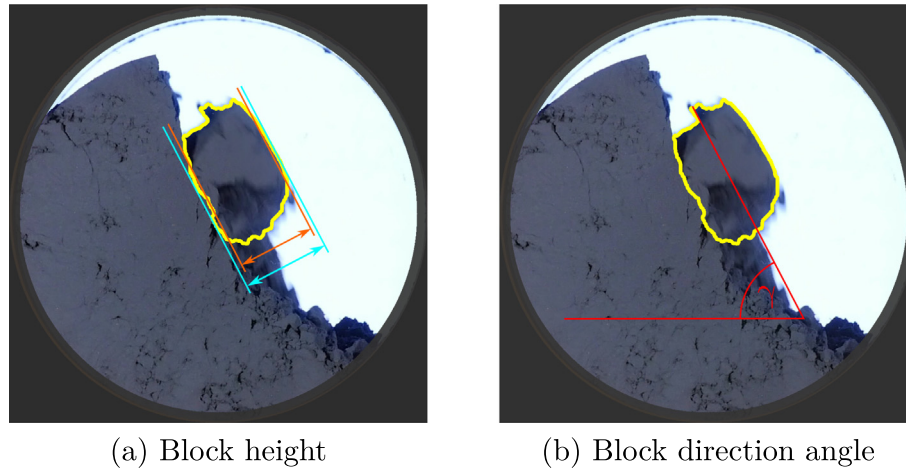| Parameter	Symbol	Bins	min	max	Class width
Block height		40	0 mm	60 mm	1.5 mm
Block width		40	0 mm	103 mm	2.575 mm
Top edge height		40	0 mm	103 mm	2.575 mm
Block speed		40	0 mm s^{-1}	900 mm s^{-1}	22.5 mm s^{-1}
Block direction		40	0°	90°	2.25°
Block rotation		40	−5.0 s^{-1}	15.0 s^{-1}	0.5 s^{-1}

(a) Block height

(b) Block direction angle

Fig. 3. Illustration of the block detection method. The block height (a) is given by the size of the contour perpendicular to the mean velocity. The overall measurement which is susceptible to outliers, is shown in cyan. The statistical measurement, where 98% of the contour's area lie inside is displayed in orange. The block direction (b) is obtained from the direction of the mean velocity and is shown as angle γ in red.

around the mean contour. The detection of the interface can be done by thresholding the image due to the strong backlight which creates enough contrast. Afterwards, the contour around the powder bed is extracted and prepared for evaluation by removing all parts of the contour outside of a circle with a radius of 90% of the drum radius. The remaining contour approximates the interface between powder and air. An exemplary contour is displayed in Fig. 4a. This extraction is done for all frames of the video clip. Then, all interfaces are approximated by a single, linear function

$$y = kx + d \tag{3}$$

and the mean interface angle

$$\alpha_{\text{int}} = \arctan(k) \tag{4}$$

is calculated. Once the mean interface angle is known, all interfaces are rotated so that the linear fit becomes horizontal. Afterwards, a sliding window along the fitted line is used to analyze the positions of the interface for mean and deviation. The resulting mean interface, as well as the deviation, are displayed in Fig. 4b. Finally, the deviation is averaged over the whole interface to create one numeric value. This method provides

two values, the mean interface angle and the mean interface deviation, but also the mean interface contour can be seen as an output.

3. Experimental setup

For the experimental investigation of the block-like movement, we built a rotating drum setup. The drum consisted of the cylindrical part and the two covers, which were 3D-printed from polylactic acid (PLA). The main cylinder had an inner diameter $D = 103$ mm and a length $L = 63$ mm. It was closed on both ends with transparent glass plates which were fixed in the covers. The influence of powder adhering to the pane was minimized by using glass instead of Plexiglass, where we had observed strong adhesion. Furthermore, we took into account that the distance between the two panes played a decisive role. For too small values, the powder would no longer slip on the bed but, wedged between the two plates, lift off to positions which it could otherwise not reach at all.

The two covers were screwed on the cylindrical part and the drum was sealed with O-rings between the cylinder and the glass plates. To allow for a well-defined surface inside the drum, the cylinder wall was covered with self-adhesive aluminum foil. As a result, the powder did
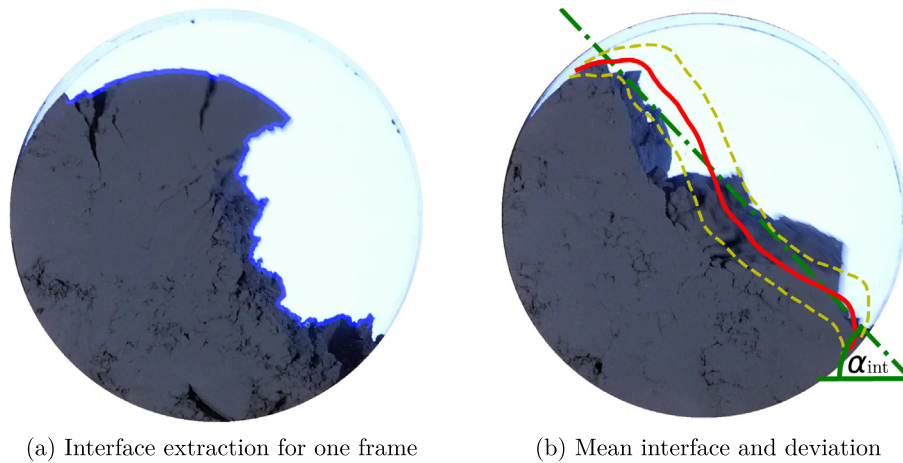

(a) Interface extraction for one frame

(b) Mean interface and deviation

Fig. 4. Example for interface extraction and evaluation. The left image shows an exemplary frame with the recognized interface. In the right image, the green line represents the linear function fitted to the mean interface highlighted in red. The deviation around the mean interface is displayed in yellow.
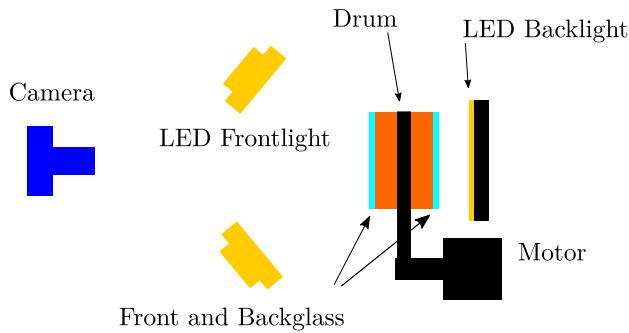
Fig. 5. Schematic of the rotating drum experimental setup. The cylindrical drum unit with transparent cover plates sits in front of a backlight and is connected to the motor by a timing belt. Two additional LED spots illuminate the front of the drum unit to have a high quality view for the camera which sits on the rotation axis of the drum.

not come into contact with the plastic surface. The main platform held four wheels to guide the drum and enabled a smooth rotation. The motor was situated below these wheels and connected to the drum via a timing belt. To have good control over the rotational speed, we employed a stepper motor of the NEMA-17 size. The front of the drum was illuminated by two 6 W LED spotlights while, a 16×16 WS2812B RGB-LED-panel with a diffuser foil was used as backlight. The behavior of the powder was filmed by a Panasonic Lumix DMC-GH4, a Micro Four Thirds System digital still and video camera at 96 fps with a resolution of 1920×1080 positioned on the rotation axis of the drum. To minimize the perspective effect, it was positioned 1500 mm away from the drum with the focus set up in such a way that the focal point was behind the front glass. The drive was regulated by a stepper motor controller connected to a microcontroller board which did the speed ramping and ensured smooth rotation. The board was connected to a PC which ran a software for motor and camera control. A sketch of the setup is shown in Fig. 5.

3.1. Experimental procedure

The drum was filled with a defined mass of powder, which was determined by evaluating the bulk density and calculating the required mass to fill half of the drum volume. The bulk density for cohesive powders is strongly connected to the consolidation state. Therefore, the evaluated density depended on the specifics of the procedure. The filling amounts were chosen such that the powders showed a visual filling degree of about 0.6. After the drum unit was closed with the top cover, it was put on the four wheels, connected to the motor, and spun up to the desired rotation speed. Since capillary nucleation [24] could affect the powder if it was at rest in the drum too long, we tried to keep the time between the filling process and the start of the measurement as short as possible. Furthermore, our procedure included some rotations before the actual data collection began, which reduced the influence of the mentioned effect because the material loosened.

Two basic measurement cycles were used, the constant rotation speed mode and the rotation speed stepping mode. For the constant mode, a rotation speed of 8 rpm was selected because it turned out to be a good compromise where the block movement and breakage were sufficiently prominent for the target powders, and the occurrence of the events was at an acceptable rate to keep observation times low. For the constant rpm mode, four consecutive runs with five rounds each, without interrupting the rotation of the drum and only small pauses between the four cycles, were done. For the stepping mode, the speed was changed in steps from 2 – 24 rpm. Each change in rotation speed was done by ramping to have a smooth transition and was followed by a waiting time to ensure that the motion inside the drum stabilized.

Several other authors used quite low rotation rates to picture avalanche behavior [14,17,18]. Pleass and Jothi [17] stated values as low as 0.3 rpm. Other works employed somewhat faster rotation rates similar to ours: Alexander et al. [12] reported on a 140 mm diameter cylinder at 7 rpm, Shi et al. [4] operated the GranuDrum at 1 to 10 rpm and Chou and Hsiau [25] chose 1 to 4 rpm with a 300 mm diameter cylinder. With these numbers in mind, the chosen range of speeds in this work was reasonable to visualize and analyze the dominant block-like motion of powder caused by strong cohesive forces. The value for our constant speed test was similar to that of Alexander et al. [12]. While lower speeds would have increased observation time, higher ones would have led to a situation where the effects of cohesion would have been less visible and were therefore not investigated.

To classify the range of speeds, we used the Froude number which can be defined as

$$Fr \equiv \frac{\omega^2 R}{g}, \tag{5}$$

with the angular velocity ω, the inner radius of the drum R, and the gravitational acceleration g. The employed rotation rates corresponded to values from $Fr = 2.3 \cdot 10^{-4}$ to $Fr = 3.3 \cdot 10^{-2}$. According to the flow regimes listed by Mellmann [26], this ranged from rolling to cascading motion. The rotation speed of the constant speed test (8 rpm) with $Fr = 3.7 \cdot 10^{-3}$ lay in between the two regimes.

In principle, five laps were recorded for each rotation speed, but an upper and lower time limit of 30 and 75 s was used. This ensured that on the one hand, the amount of data was kept within reasonable limits, and on the other hand, a reasonable duration was recorded at higher speeds.

The whole evaluation process for a video clip of a constant speed test at 8 rpm using five rounds of rotation took about one hour. Most of the time was used for the evaluation of the optical flow analysis with a Nvidia Geforce 2070. This step was rather storage intensive, and the used computer suffered from little storage performance. Hence, there is definitely room for improvement to speed up the whole process with higher-level hardware.

4. Results

We conducted tests with two different, strongly cohesive metal powders (in the following referred to as M1 and M2) with similar particle sizes but different flow properties and a third, mildly cohesive powder M3 with better flowability, to demonstrate the general applicability of the described characterization method. The size of the particles for all three powders was in the low micrometer range, where M3 consisted of the largest and smoothest grains, which caused weaker cohesion forces. Other, recently discussed mechanisms [27,28] such as specific, bimodal size distributions played no role in our case. First, the influence of the filling amount of the drum on the final characterization results was evaluated. Afterwards, the materials were characterized in constant speed and speed stepping mode. Finally, we showed the changes due to preconditioning the powders in different relative humidity.

4.1. Sensitivity of the measurements on the filling amount

Cohesive powder materials reach their final bulk density only after some rotations in the drum, which makes it difficult to exactly match a desired filling degree. For this reason, we evaluated how the mass in the drum influenced the measurements to check the importance of precise filling. Therefore, experiments with different mass loadings of M1 powder were performed. First, a test with nominal filling was done, followed by several tests with adding or removing small amounts of the material. The nominal filling was determined as described in Sec. 3.1. Note that the change of the material due to the rotations of previous

Table 2
Deviation data for the filling amount test. The changes are based on the average between the first and the last test, done with original filling. Lower and upper bound show the extreme values for all tests. To estimate the time behavior, the change from the first to the last test is reported.

Parameter	Lower bound	Upper bound	Change over time
Block height	−1.9%	+2.6%	+3.8%
Block width	−1.1%	+3.0%	+1.5%
Block direction	−4.7%	+2.14%	−4.3%
Block top edge height	−5.0%	+1.4%	+0.5%
Block speed	−2.3%	+2.8%	−1.2%
Block rotation	−10.8%	+5.8%	−11.7%
Interface angle	−1.8%	+0.9%	−1.7%
Interface deviation	−1.9%	+2.6%	3.6%
Visual filling degree	−20.9%	+8.5%	−0.7%

tests and the longer exposure to the atmosphere were additional influence factors that could not be removed easily. To quantify the change of the powder during measurement time, we carried out a final test with the original filling amount. The filling ratio is defined as

$$\text{filling ratio} \equiv \frac{\text{filling mass}}{\text{nominal filling mass}}. \tag{6}$$

Configurations from 75% to 110% filling ratio were investigated. For the numerical evaluation of the variation, the average of the first and the last test was used as the basis. The minimal and maximal deviations are reported in Table 2. Additionally, the variation over time is provided to estimate the influence of material change and better separate these factors.

For most block properties, there was little influence of the filling amount, and no clear trends could be identified. Only the visual filling degree displayed in Fig. 6a depended almost linearly on the drum loading as was to be expected, and the block top edge value in Fig. 6b also followed a linear, but rather weak dependence. For the other block variables, no clear trend could be obtained as shown exemplarily for block height (weak influence) and rotation (medium, but irregular influence) in Fig. 6c and d.

Similarly, the interface values also provided in Table 2 exhibited only a weak dependence on the drum loading. The mean interface angle tended to have a slightly lower value for higher filling amounts, while for the interface deviation, the opposite was the case.

The largest variations were found in the block rotation ranging from −10.8% to +5.8%. Notably, these changes accumulated nearly monotonic in time (not explicitly shown here), so the dependence on the history and/or the environment was more prominent than that on the drum loading. More specifically, we found a change over time of −11.7%, which could nearly explain the whole change for all filling amounts. Hence, the block rotation might serve as a quite sensitive measure for the current powder state. We conclude that the mass of powder in the drum (as long as it is within reasonable bounds) does not have a significant impact on most of the block analysis results, but its history and environmental factors can play an important role.

4.2. Characterization of two different strongly cohesive powders

Next, we used the block analysis method to characterize M2 powder with better and M1 with worse flow properties and outline their differences. We used both the constant rotation and the speed stepping test. Afterwards, we estimated the changes due to preconditioning of the powder with the constant rotation speed test to point out the sensitivity of this method.

4.2.1. Drum test with constant rotation speed

We started our measurements with the constant speed test. A selected subset of the most important distributions of the estimated characteristic block values is displayed in Fig. 7. The small deviation of the

distributions showed that the method had converged in little observation time: One measurement consisted of only five rotations of the drum. Each of the four measurements alone would have provided enough information for the characterization of the investigated powders.

We could observe significant differences between M1 and M2. First, the block height distribution for M1 powder was broader with a significantly higher mean value than for M2. The block width instead showed only a minor difference with the tendency for M2 to have blocks with a width in the range of 40–60 mm more frequently. The M2 powder had a more narrow distribution of the block direction angle with a lower mean value than M1 powder. We observed a significantly more stable, rigidly moving part of M1 in the distribution of the block top edges (not shown), which implied higher blocks for this material and consequently higher velocities. While M2 only reached velocities up to 400 mm s^{-1}, M1 went up to over 600 mm s^{-1}. Finally, less rotation of the block structures could be observed for M2 (not shown).

Altogether, the constant speed test was able to identify significant differences between the two materials. For both of them, the distribution functions showed stable results with low deviation around the mean of repeated runs.

4.2.2. Drum test with different rotation speeds

Besides the constant rotation test, we investigated the response of our two powders to different rotation speeds. We started at a low value of 2 rpm and increased it in steps up to 24 rpm. The changes of the mean block height, width, direction, and speed can be seen in Fig. 8. For M1, the mean block height displayed in Fig. 8a clearly increased with the rotation speed. For M2, a similar observation at a different base level was made for low rotation rates. However starting from 10 rpm, a more prominent increase occurred. We speculate that the stronger centripetal force at higher rotation rates together with increased fracturing and subsequent stronger material compaction gave rise to this behavior. Fig. 8c shows that the block width of both materials increased pronouncedly above rotation speeds of 10 and 16 rpm, respectively. Below these values, both powders underwent only a slight increase from 43 mm to approximately 50 mm. These breakaway points indicated the rotation rates where the flows developed away from clearly separable avalanche events with pauses in between to a behavior that was also avalanche based, but with more frequent events so that some powder blocks were always in motion relative to the drum.

The direction (Fig. 8b) of M1 blocks followed a slight, nearly linear decrease with increasing rotation rate. At 2 rpm, M2 powder showed an angle that was marginally above the value of M1, but it was subject to a somewhat stronger decrease in angle until 16 rpm and flattened out afterwards. This was contrary to the expectation for cohesionless materials, but can be explained with the increased block height for higher rotation rates (see above).

For the block speeds in Fig. 8d, only minor changes with angular frequency could be seen for each of the two powders. However, particularly for the block speed, a significant difference between the materials was observed, which had also presented itself in the constant speed test. Finally, the block top edge height and the block rotation (not shown) were hardly influenced by the rotational speed and quite similar for both materials.

To compare the block to the interface analysis method, the mean interface deviation and the mean interface angle for the different rotation speeds are additionally shown in Fig. 8a and Fig. 8b. A very similar behavior of the interface and the block values, especially of the deviation and the block height, was found below the breakaway point. Above, the two measures started to deviate: The interface deviation stayed at the same level, but the block height increased further. This can be attributed to the fact that the block height started to describe the thickness of the whole flow region while the interface deviation did not take the regions where continuous motion occurred into account. A different behavior was observed for the interface angle in Fig. 8b, which became
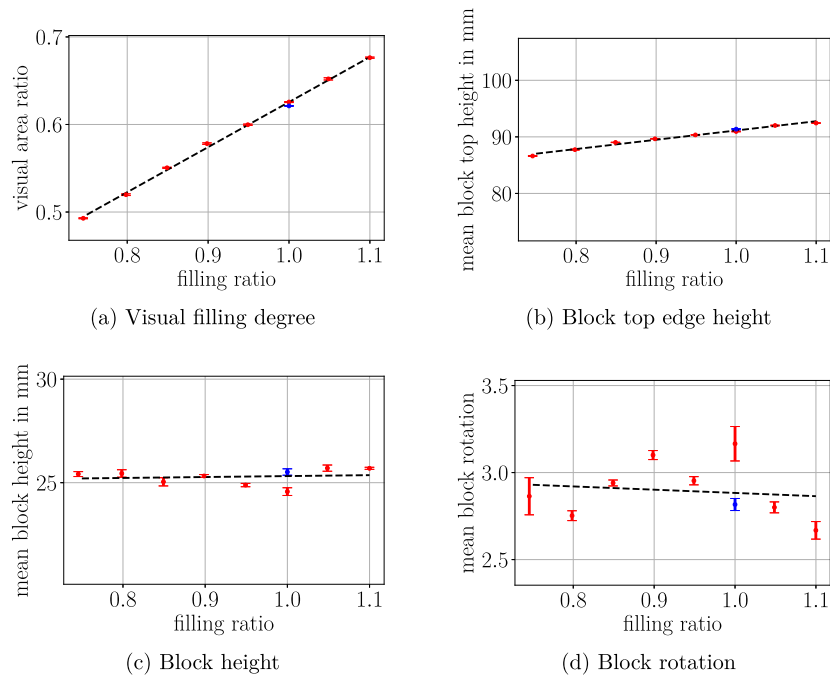
(a) Visual filling degree

(b) Block top edge height

(c) Block height

(d) Block rotation

Fig. 6. Results of the block evaluation of the filling degree test. The filling ratio is defined as fraction of current filling mass over nominal filling mass. The Y-axis scaling is adopted for 20% changes around the average. For pointing out the trend, a linear function was fit to the data points. However, this does not imply that the underlying physical effect or dependency is necessarily of linear nature. The validation step with nominal filling is shown in blue.
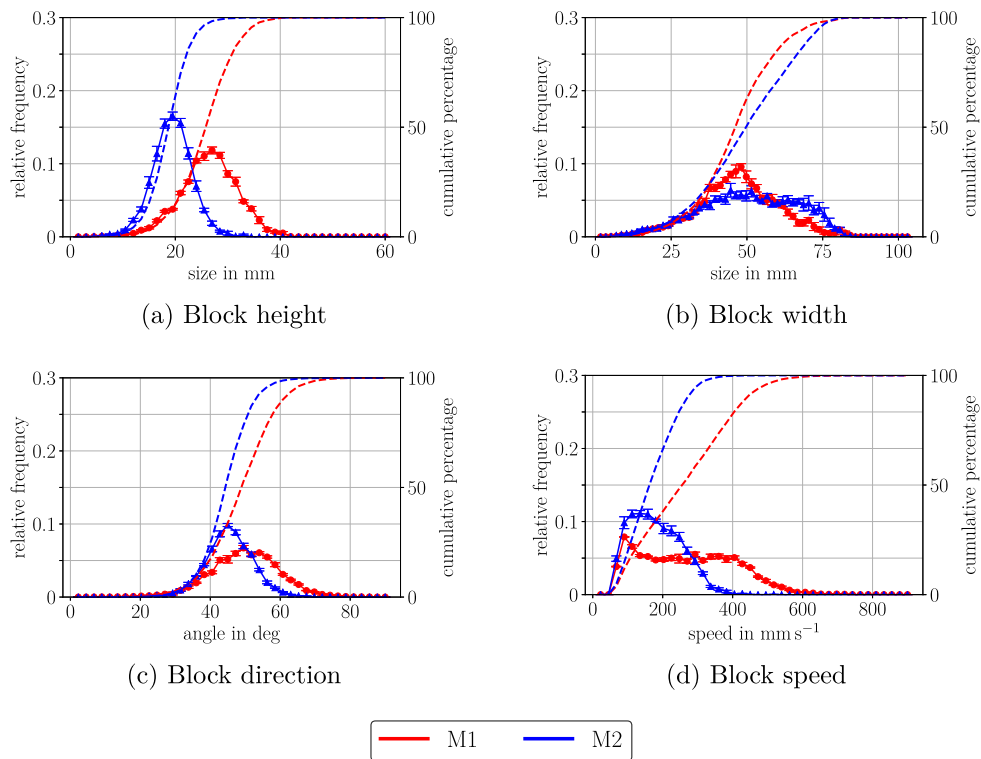

(a) Block height

(b) Block width

(c) Block direction

(d) Block speed

Fig. 7. Distributions of the block measurements from the constant speed test for M1 (red) and M2 (blue). The solid line with the error bars shows the relative frequency (all data points sum to 1) and the dashed line corresponds to the cumulative distribution. The error bars visualize the standard deviation of the mean that was calculated from four individual tests.
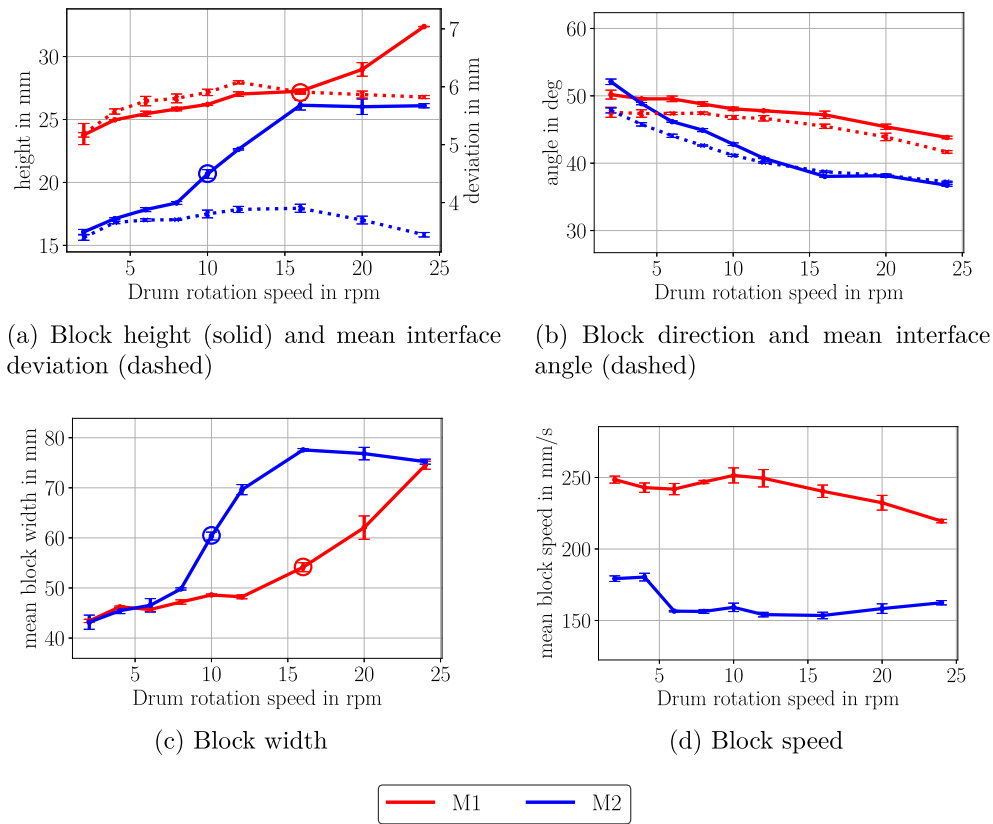
(a) Block height (solid) and mean interface deviation (dashed)

(b) Block direction and mean interface angle (dashed)

(c) Block width

(d) Block speed

Fig. 8. Block values over rotation rate from the speed stepping test for M1 (red) and M2 (blue). In the first two diagrams, the values from the interface evaluation are added and the breakaway points are marked with circles. The error bars visualize the standard deviation calculated from three samples.

very similar to the block direction for higher rotation rates. This was not surprising because the two measures describe the same property when strongly block-like movement disappears.

The speed stepping test pointed out that the structures increased in size with increasing rotation speed. We could also observe that the flow changed qualitatively above specific rates: Below, clearly separable avalanche events with pauses of no motion were seen, and above, it developed to a flow with such regular avalanches that there was always some moving material. For M2 powder, already 8 rpm posed an upper bound to the strongly avalanche-dominated flow.

Besides the possible usage of the transition speed as an additional characterization parameter, this test is also important for choosing an appropriate speed in the constant speed test and for determining the regime in which the analysis is done.

4.3. Characterization of a mildly cohesive powder

To extend the range of investigated cohesion levels, we applied our methodology to a powder with weaker cohesion. Here, we used a better
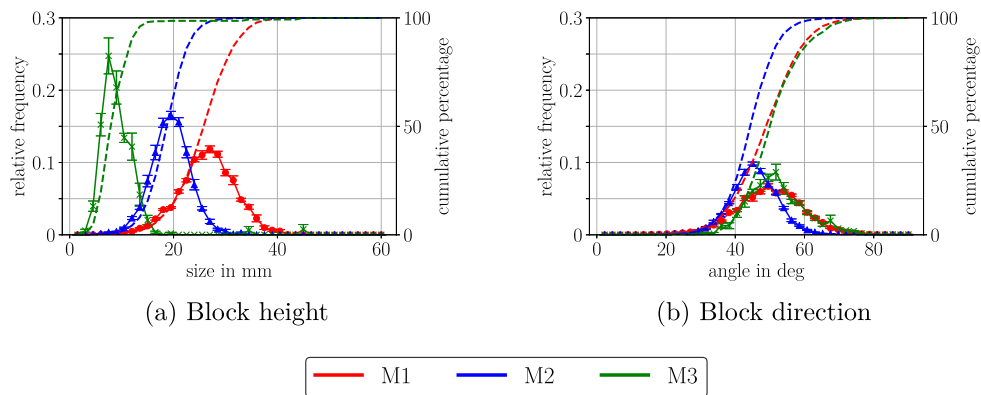

(a) Block height

(b) Block direction

Fig. 9. Distributions of the block height and direction for M3 powder (green) from a constant speed test. Additionally, the results for M1 (red) and M2 (blue) are added as reference. The line with the error bars shows the relative frequency (all data points sum to 1). The error bars visualize the standard deviation of the mean that was calculated from four samples.

flowing metal powder (M3) intended for additive manufacturing. The resulting distributions of the block height and the block direction are shown in Fig. 9 in combination with the results for M1 and M2 as reference. The lower cohesion of this material is especially noticeable in the block height visualized in Fig. 9a. The M3 powder led to a block height distribution shifted to significantly smaller values than observed for both M1 and M2 with an average of approximately 10 mm. On the contrary, the distribution of the direction of the blocks (Fig. 9b) of M3 powder was quite similar to the distribution for M1 powder.

Even though the distributions for M3 were subject to somewhat larger variances than those for M1 and M2, the curves were sufficiently smooth to be used for material characterization. Our method can hence be used not only for strongly cohesive powders which are the actual, challenging target system but also for mildly cohesive ones.

4.4. Characterization of preconditioned powder

For any characterization method, it is important to capture as many properties of the material as possible. In the following, this is demonstrated by the evaluation of the influence of environmental factors like humidity. Therefore, we preconditioned M1 powder in cans with specific relative humidity (RH) and analyzed it after a fixed period of time. In this experiment, we used five different levels of <5%, 20%, 40%, 60%, and 80% RH at 20 °C. The RH value for a drying can with silica gel is referred to as 0%. The powder was stored in the humidification setup for 90 h, then the samples were tested and returned to the humidification setup. After another exposure period of 70 h, the samples were tested again. We recorded changes relative to the results from the constant speed test of the fresh material. Diagrams for the change in block height, speed, rotation, and interface deviation can be found in Fig. 10.

After the first humidification period, block height, speed, and interface deviation exhibited a monotonic increase with increasing humidity. The more humid the powder, the larger and faster were the observed blocks and led to a higher interface deviation. In general, the effect was strongest for dried material with changes of about −15% but also clearly visible for 80% RH with changes of 5% and more. Only block rotation did not follow such a simple trend and was strongly increased by 10% to 30% for all humidities including the dried sample.

After the second period, the block height and interface deviation decreased for almost all humidities compared to the first period and also to the fresh material. Only the interface deviation at high humidities was similar to that of the fresh powder (after having been enhanced after the first period).

The block speed as well as the rotation showed the most significant changes due to the humidification procedure. Speeds of the blocks in the dried sample were reduced by nearly 25% while those for the sample stored at 80% RH increased by nearly 25%. There was also a distinct change in the rotation behavior after the second humidification period. The dried sample was reduced by over 30% while the sample stored at 80% RH showed an increase of over 50%.

The importance of these two additional measures is demonstrated by the sample stored at 80% RH. Although the visual behavior was completely different compared to before preconditioning, no differences in the block height (Fig. 10a), the interface deviation (Fig. 10b), the interface angle (not shown) or the block direction (not shown) could be observed. We also studied the shape of the interface, but for this specific case, we could not find any useful difference, either. In contrast, block speed and rotation were highly sensitive to the change of material dynamics. This indicates that only considering the interface angle and deviation or single block properties is not enough to fully characterize the state of such a metal powder. We get a much more
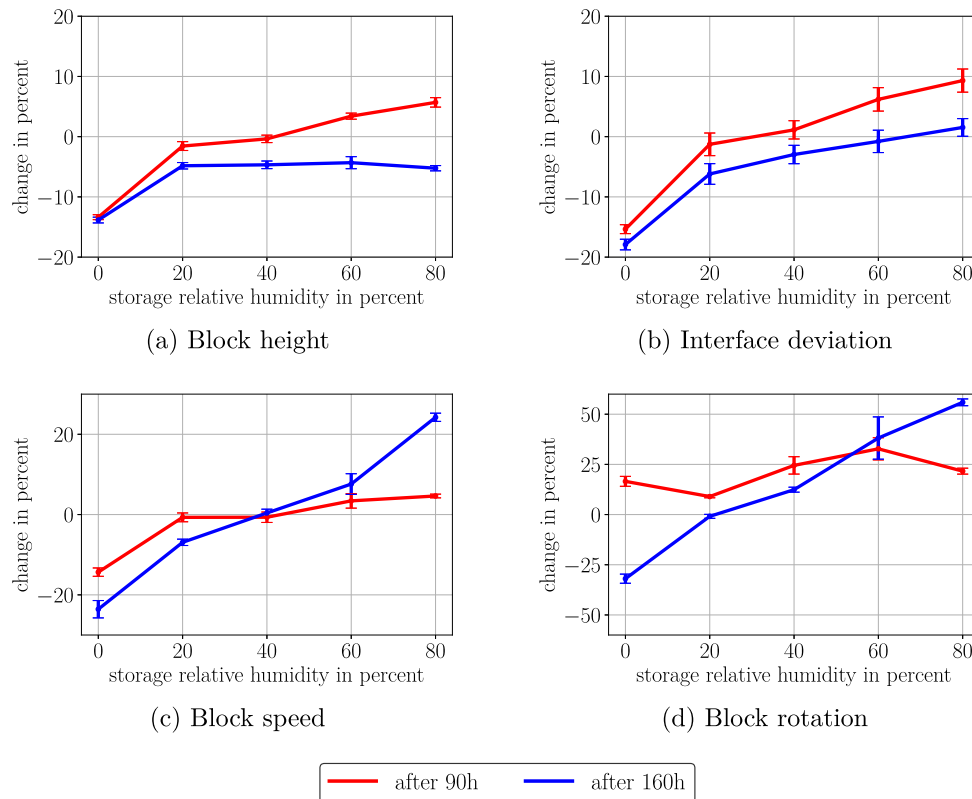

(a) Block height   (b) Interface deviation

(c) Block speed   (d) Block rotation

— after 90h   — after 160h

Fig. 10. Block values with preconditioned powder from the constant speed test with M1 powder. The test results after the first humidification period are shown in red and those after the second period in blue. The markers visualize the standard deviation that was calculated from two samples.

detailed view of the flow behavior with the complete block evaluation method. Notably, not only did it detect the influence of preconditioning over no such procedure. It also showed that the results for two different exposure times to humidity differed significantly. This suggests that, apart from the direct effect of moisture, there was another process that had an impact on the flow behavior. We suspect an oxidation reaction, but it would take a more detailed investigation to answer this question.

4.5. Comparison with existing methodology

Finally, we want to comment on the relationship of our novel block analysis with the well-known interface evaluation method. Since not all details are publicly available, we re-implemented the approach along the lines of Lumay et al. [2] as described in Sec. 2.2. Our version used all 3600 snapshots from the constant speed test, fitted the interfaces of all frames at once, and evaluated the deviation perpendicular to the linear fit. As discussed below, this made it statistically more robust for strongly cohesive materials than the original one which included only 50 frames with 0.5 s spacing. In order to compare the two approaches, we employed the mean block height and the mean block direction from the constant speed test in Sec. 4.2. We calculated for each measure and material the relative deviation (based on the mean value) for the four tests and the average between the two materials to get a more universal image. This resulted in an average deviation of 1.5% for the block height, 1.1% for the block direction, 1.7% for the interface deviation, and 0.5% for the interface angle. Hence, all quantities exhibited a similarly low scattering. Notably, the originally proposed smaller number of frames led to a significantly higher deviation for the interface deviation of 4.3%, which could be large enough so that two different material flow states might not be distinguishable. Nevertheless, both approaches delivered results with low scattering if high enough sampling rates were used. They converged after 20 s — 25 s at 8 rpm, which was drastically faster than methods that rely on avalanches observed at very low rotation rates. Hence, our technique is at least as statistically robust and efficient as already established methods, but its main advantage is the higher sensitivity that allows it to detect even small differences in material properties.

5. Conclusion and outlook

In this work, we developed a block-movement-based analysis method for cohesive powders in a rotating drum. This has proven to be a stable, reproducible, and efficient approach.

We carried out the block analysis for two strongly cohesive metal powders M1 and M2 at constant speed and with a rotation speed sweep. We observed significant differences between them, especially concerning the block size and speed. M1 and M2 behaved completely differently at the rotation speed sweep, most notably in terms of different breakaway rotation rates where the flow turned from individual-avalanche-based to a more continuous form. Additionally, we investigated a third material M3 with weaker cohesion forces and hence quite different flow properties. Our method could easily discern all three substances. Finally, to induce some variation in the behavior of the M1 powder, we preconditioned it at different humidity levels. We stress that the block analysis method showed a significantly higher sensitivity towards these humidity-induced changes in flowability by combining various characteristic parameters as opposed to approaches that describe the material behavior with only one or two parameters.

By taking into account the entire life cycle of an avalanche, our method provides more information about the behavior of a powder on the one hand (which allows to identify even small differences), and it converges quickly on the other hand. Hence, stable results can be gained in less observation time. Consequently, our approach seems to be a promising candidate for detecting changes in the flow properties of such powders and for the comparison of measurement data with the

results of a DEM simulation. This is of major interest for the further usage of calibrating DEM model parameters for cohesive powders under low consolidation stress. Therefore, we will extend the methodology to be directly applied on simulation data in future work.

In good academic spirit, we want to point out a current weakness of our method which lends itself to future improvements. Currently, all contiguous contours are considered block candidates even though a recognized contour may consist of multiple physical blocks. With a more sophisticated segmentation process, the contour may be split into the physical blocks of the material. We tested several approaches from segmentation by velocity magnitude to exploiting the different rotation values of the individual blocks by the usage of a velocity pole estimation. None of the tested approaches could provide sufficiently stable segmentation results to be used for characterization. Therefore, we omitted segmentation and assumed that each connected contour represented a block.

Finally, it would be interesting to perform an in-depth comparison to other characterization techniques like direct shear testing with a variety of different powders to investigate which parameters are dominant in the individual measurement tools and to shed light on the impact of consolidation on the material flow behavior.

Supplementary data to this article can be found online at https://doi.org/10.1016/j.powtec.2022.117209.

Credit authorship contribution statement

T. Kronlachner: Methodology, Investigation, Writing – original draft. **S. Pirker:** Conceptualization, Project administration, Funding acquisition. **T. Lichtenegger:** Methodology, Writing – review & editing, Supervision.

Declaration of Competing Interest

The authors declare that they have no known competing financial interests or personal relationships that could have appeared to influence the work reported in this paper.

Acknowledgment

References

[1] J. Schwedes, Review on testers for measuring flow properties of bulk solids, Granul. Matter 5 (1) (2003) 1–43.

[2] G. Lumay, F. Boschini, K. Traina, S. Bontempi, J.C. Remy, R. Cloots, N. Vandewalle, Measuring the flowing properties of powders and grains, Powder Technol. 224 (2012) 19–27.

[3] C. Meier, R. Weissbach, J. Weinberg, W.A. Wall, A. John Hart, Modeling and characterization of cohesion in fine metal powders with a focus on additive manufacturing process simulations, Powder Technol. 343 (2019) 855–866.

[4] H. Shi, G. Lumay, S. Luding, Stretching the limits of dynamic and quasi-static flow testing on cohesive limestone powders, Powder Technol. 367 (2020) 183–191.

[5] M. Ghadiri, M. Pasha, W. Nan, C. Hare, V. Vivacqua, U. Zafar, S. Nezamabadi, A. Lopez, M. Pasha, S. Nadimi, Cohesive Powder Flow: Trends and Challenges in Characterisation and Analysis, KONA Powder Part J. 37 (2020) 3–18.

[6] A.W. Jenike, Storage and flow of solids, bulletin no. 123, Bull. Univ. Utah 53 (26) (1964).

[7] ASTM D6773 - 16, Standard Test Method for Bulk Solids Using Schulze Ring Shear Tester, Standard, ASTM International, West Conshohocken, PA, 2016.

[8] R. Freeman, Measuring the flow properties of consolidated, conditioned and aerated powders - A comparative study using a powder rheometer and a rotational shear cell, Powder Technol. 174 (1–2) (2007) 25–33.

[9] L. Zhang, Z. Jiang, F. Weigler, F. Herz, J. Mellmann, E. Tsotsas, PTV measurement and DEM simulation of the particle motion in a flighted rotating drum, Powder Technol. 363 (2020) 23–37.

[10] T. Nijssen, M. Van Dijk, J. Kuipers, J. Van der Stel, A. Adema, K. Buist, Experiments on floating bed rotating drums using magnetic particle tracking, AICHE J. (2022) In press.

[11] E.R.L. Espiritu, A. Kumar, A. Nommeots-Nomm, J.A.M. Lerma, M. Brochu, Investigation of the rotating drum technique to characterise powder flow in controlled and low pressure environments, Powder Technol. 366 (2020) 925–937.

[12] A.W. Alexander, B. Chaudhuri, A.M. Faqih, F.J. Muzzio, C. Davies, M.S. Tomassone, Avalanching flow of cohesive powders, Powder Technol. 164 (1) (2006) 13–21.

[13] A. Jarray, V. Magnanimo, S. Luding, Wet granular flow control through liquid induced cohesion, Powder Technol. 341 (2019) 126–139.

[14] M. Wojtkowski, O.I. Imole, M. Ramaioli, E. Chaóvez Montes, S. Luding, Behavior of cohesive powder in rotating drums, AIP Conf. Proc. 1542 (2013) 983–986.

[15] N. Jain, J.M. Ottino, R.M. Lueptow, An experimental study of the flowing granular layer in a rotating tumbler, Phys. Fluids 14 (2) (2002) 572–582.

[16] C.E. Davies, S.J. Tallon, K. Fenton, N. Brown, A. Williams, A New approach to monitoring the movement of particulate material in rotating drums, Dev. Chem. Eng. Min. Process 12 (3–4) (2004) 263–275.

[17] C. Pleass, S. Jothi, Influence of powder characteristics and additive manufacturing process parameters on the microstructure and mechanical behaviour of Inconel 625 fabricated by selective laser melting, Addit. Manuf. 24 (2018) 419–431.

[18] Ž. Trpĕlková, H. Hurychová, M. Kuentz, B. Vraníková, Z. Šklubalová, Introduction of the energy to break an avalanche as a promising parameter for powder flowability prediction, Powder Technol. 375 (2020) 33–41.

[19] G. Bradski, The OpenCV Library, Dr. Dobb's j. softw. Tools, 2000.

[20] A. Bar-Haim, L. Wolf, Scopeflow: Dynamic scene scoping for optical flow, Proc. IEEE Comput. Soc. Conf. Comput. Vis. Pattern Recogn. (2020) 7998–8007.

[21] D. Sun, X. Yang, M.-Y. Liu, J. Kautz, Pwc-net: Cnns for optical flow using pyramid, warping, and cost volume, Proc. IEEE Comput. Soc. Conf. Comput. Vis. Pattern Recogn. (2018) 8934–8943.

[22] J. Hur, S. Roth, Iterative residual refinement for joint optical flow and occlusion estimation, Proc. IEEE Comput. Soc. Conf. Comput. Vis. Pattern Recogn. (2019) 5747–5756.

[23] W. Thielicke, R. Sonntag, Particle image velocimetry for MATLAB: accuracy and enhanced algorithms in PIVlab, J. Open Res. Softw. 9 (2021) 1–14.

[24] L. Bocquet, E. Charlaix, S. Ciliberto, J. Crassous, Moisture-induced ageing in granularmediaandthekinetics of capillary condensation, Nature 396 (1998) 735–737.

[25] S.H. Chou, S.S. Hsiau, Experimental analysis of the dynamic properties of wet granular matter in a rotating drum, Powder Technol. 491–499 (2011).

[26] J. Mellmann, The transverse motion of solids in rotating cylinders-forms of motion and transition behavior, Powder Technol. 251–270 (2001).

[27] Y.C. Chung, C.C. Liao, Z.H. Zhuang, Experimental investigations for the effect of fine powders on size-induced segregation in binary granular mixtures, Powder Technol. 387 (2021) 270–276.

[28] C.C. Liao, S.F. Ou, S.L. Chen, Y.R. Chen, Influences of fine powder on dynamic properties and density segregation in a rotating drum, Adv. Powder Technol. 31 (4) (2020) 1702–1707.